

X-RAYS FROM QUASARS AND ACTIVE GALAXIES *

Alan P. Lightman
Harvard-Smithsonian Center for Astrophysics

I. INTRODUCTION

There is evidently a great deal of activity and commotion in deep space, unrevealed by the naked eye or the delicate twinkling of the stars. As far as we can tell, quasars (QSOs) and "active galactic nuclei" (AGN) have relatively enormous power outputs produced in very small volumes. A typical quasar can produce a hundred to a thousand times the luminosity of a normal galaxy from a region one hundred thousand times smaller in size. Roughly speaking, if the city of Boston were a galaxy in terms of its power output and size, then a quasar would have the power of the entire United States produced in a region the size of a baseball.

At various times, it has been suggested that new kinds of physical laws or phenomena must be required to explain these objects. But more and more evidence has accumulated that shows a continuous range of energetic activity, starting with normal galaxies, going through Seyfert galaxies and other AGN, and joining with the less luminous quasars. Moreover, the hypothesized model of gas falling through a deep gravitational well, probably caused by a massive black hole, together with a net angular momentum in the bottom of the well, seems capable of explaining, at least qualitatively, the full range of observed phenomena, from the energetics to the striking, long-lived "jets" of matter observed to ema-

*Based on a lecture given at the Goddard Workshop on X-ray Astronomy (October 1981).

nate from the centers of these objects. In any case, there does seem to be good evidence for some universality in the mechanisms and physical conditions.

Among the most important issues in understanding QSOs and AGN are (1) the nature of the power source, (2) the radiation processes, and (3) the mechanism for formation and collimation of the jets. We will discuss these issues in turn, giving a brief, model-independent sketch of some of the important theoretical ideas and observations (with more emphasis on our own interests), and suggesting future work. It is possible that no new observations within the foreseeable future will satisfactorily pin down the above issues.

We will be particularly concerned with phenomena that produce X-rays. The clear association of strong X-rays with QSOs and AGN and the rapid time variability seen in X-rays indicate that this region of the spectrum may contain much information about the conditions near the central region of the objects. Of course, simultaneous observations of all regions of the spectrum may provide important clues to the mechanisms at work.

For some recent reviews of this subject, see e.g. Rees (1977,1978,1980), Fabian and Rees (1979), and Bradt (1980).

II. NATURE OF THE POWER SOURCE: ACCRETION ONTO A MASSIVE BLACK HOLE

A. General Considerations

We will tentatively adopt gas accretion onto a massive black hole as the "standard model" for the power source. The

length scale is then set by the Schwarzschild radius of the black hole, $r_g = 2GM/c^2$, where M is the mass of the hole. We will use the notation $M_B \equiv M/10^8 M_\odot$. Unless the hole is rotating near maximum angular velocity, we can expect the energy production to peak in the region $r \sim 10 r_g$. The luminosity, L , can be written as

$$L = \epsilon \dot{M} c^2, \quad (1)$$

where ϵ is the efficiency parameter and \dot{M} is the mass accretion rate. The virial temperature, T_V , set by the proton rest mass energy, is

$$T_V = 10^{12} \text{K} (r/10r_g)^{-1}. \quad (2)$$

The period of a circular orbit, P , also denoted by t_K , in the Newtonian approximation, is

$$P = t_K = 3 \times 10^5 \text{s} M_B (r/10r_g)^{3/2}. \quad (3a)$$

The light travel time across this region is

$$\Delta t_L \equiv r/c = 10^4 \text{s} M_B (r/10r_g). \quad (3b)$$

The total mass accreted, M_{acc} , in the active lifetime, t_{life} , is

$$M_{acc} \equiv \dot{M} t_{life} = 10^7 M_\odot \left(\frac{t_{life}}{10^8 \text{yr}} \right) \left(\frac{L}{10^{45} \text{erg s}^{-1}} \right) \left(\frac{\epsilon}{0.1} \right)^{-1}. \quad (4)$$

Both the combination of inferred active lifetimes and observed luminosities, and the sizes and velocity dispersions obtained from optical studies, indicate an M_{acc} and an M in the range $10^6 - 10^9 M_\odot$. We denote the ratio of radial velocity, V_r , to Kepler velocity, V_K , by

$$\beta \equiv V_r / V_K. \quad (5a)$$

The radial infall time, t_r , is then

$$t_r = t_K / \beta. \quad (5b)$$

Note that β is related to the viscosity parameter α of the

ORIGINAL PAGE IS
OF POOR QUALITY

" α -model" disks (Shakura and Sunyaev 1973) by

$$\beta = \alpha (h/r)^2, \quad (5c)$$

where h is the disk thickness at radius r . In "thick accretion disks" we might expect $h \sim r$, so that $\beta \sim \alpha$. The continuity equation gives an ion number density, N ,

$$N = 10^{10} \text{ cm}^{-3} M_8^{-1} \left(\frac{\epsilon}{0.1}\right)^{-1} \beta^{-1} (L/L_{\text{EDD}}) (r/10r_s)^{-3/2}, \quad (6)$$

where we have normalized L in terms of the Eddington luminosity

$$L_{\text{EDD}} \equiv 4\pi G M c m_p / \sigma_T = 10^{46} \text{ erg s}^{-1} M_8.$$

We will denote the mass of the proton and electron by m_p and m , respectively, and σ_T is the Thomson cross section. From equation (6) we obtain the "ion scattering depth"

$$\tau_N \equiv r N \sigma_T = 2 \left(\frac{L}{L_{\text{EDD}}}\right) \left(\frac{\epsilon}{0.1}\right)^{-1} \beta^{-1} \left(\frac{r}{10r_s}\right)^{-1/2} \quad (7)$$

The Thomson scattering depth is

$$\tau_{\text{th}} = r (n_+ + n_-) \sigma_T \gg \tau_N \quad (8)$$

where n_- and n_+ are the electron and positron number densities.

Although τ_N might be expected to approach unity in sources radiating at near the Eddington limit, equation (7), the large optical polarization seen in some QSOs and BL Lac objects (Stein, O'Dell, and Strittmatter 1976; Angel 1978), together with the as yet unobserved evidence of strong Comptonization, suggests $\tau_{\text{th}} < 1$. We then obtain an upper limit for the mass in the central, emitting region, M_{em} (Rees 1977)

$$M_{\text{em}} \equiv \frac{4}{3} \pi r^3 m_p n \ll 4 \times 10^{-4} M_0 M_8^2 \left(\frac{r}{10r_s}\right)^2. \quad (9)$$

Since $M_{\text{em}} \ll M$, most of the mass has already collapsed within the emitting region, arguing against some

non-black-hole models for the central power source. Of course, the majority of QSOs and AGN do not show strong optical polarization.

B. Gas flow models

The principal requirements for efficient conversion of gravitational energy into radiation, $\epsilon \gtrsim 0.1$, are that (a) the viscous dissipation time scale be comparable to or shorter than the radial infall time scale and that (b) the cooling time of the gas be shorter than the radial infall time scale. When angular momentum is present, an accretion disk forms; most accretion disk models proposed satisfy the above requirements. Even when the infalling gas does not have much net angular momentum, a disk may form out to a radius $r \sim 10^2 r_g$ due to the "dragging of inertial frames" by a rapidly rotating black hole (Bardeen and Petterson 1974). Spherical accretion models require rapid dissipation, since the infalling matter is not delayed by angular momentum.

For a review of the types of α -disk models, see Eardley et al. (1978). These models differ in whether they are gas or radiation pressure dominated, optically thick or thin, equal or unequal temperatures for electrons and ions, and in the source of photons; they have in common the assumption of a spatially constant value for the viscosity parameter α and the assumption of a thin disk $h \ll r$. Recently, Lynden-Bell (1978) and Jaroszynski, Abramowicz, and Paczynski (1980) have considered geometrically thick disks, but without including the effects of viscosity. These thick-disk models are characterized by an unspecified free function, $l(r)$, the

non-Keplerian angular momentum distribution along the disk. When more of the internal physics of the disk is included, this function may be determined. For some recent spherical accretion models, see Maraschi et. al. (1979) and Maraschi, Roasio and Treves (1981).

An alternative possibility, for both the matter surrounding the hole and the method of energy release, is a disk that anchors a large-scale magnetic field, torquing and spinning down a rapidly rotating black hole (e.g. Blandford and Znajek 1977). In this case the energy is supplied by the rotation of the hole. (At an earlier stage, this energy had to ultimately derive from energy made available in gravitational collapse.) Thermodynamically, this process can provide relatively low-entropy energy that is well suited for accelerating electrons to relativistic velocities.

C. Time Variability

Time variability in the X-rays of $\Delta t \sim 10^3 - 10^4$ s has now been observed in a number of QSOs and AGN. Some of these results are shown in the Table below, where the observed luminosity L_x is typically in the range 2-10 keV.

Table 1

| Source | L_x (erg/s) | $\Delta L_x/L_x$ | Δt (s) | $c \Delta t$ (cm) |
|----------|----------------------|------------------|-------------------|----------------------|
| Cen A | 1×10^{43} | 0.25 | 7×10^3 | 2×10^{14} |
| Mk 421 | 1×10^{44} | 2.0 | 1×10^5 | 3×10^{15} |
| NGC 6814 | 1×10^{43} | 1.5 | 2×10^2 | 6×10^{12} |
| OX 169 | 1×10^{44} | 1.5 | 6×10^3 | 1.8×10^{14} |
| 3C 273 | 1.7×10^{46} | 0.1 | 6×10^3 | 1.8×10^{14} |
| NGC 4151 | 5×10^{42} | 3.0 | 1×10^3 | 3×10^{13} |

The observations for Cen A are from Delvaile et al. (1978), for Mk 421 from Ricketts, Cooke and Pounds (1976), for NGC 6814 from Tennant et. al. (1981), for OX 169 and 3C 273 from Tananbaum (1980), and for NGC 4151 from Tananbaum et. al. (1978). A typical observed fluctuation is shown in Figure 1 for Ox 169.

ORIGINAL PAGE IS
OF POOR QUALITY

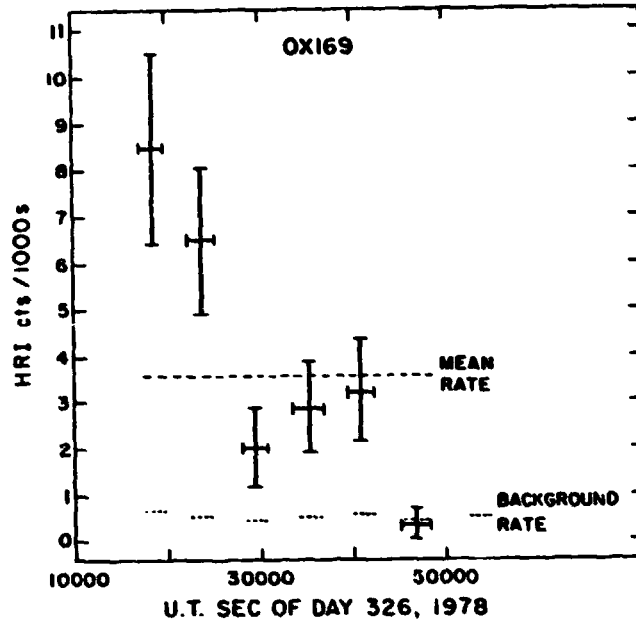


Figure 1: Einstein HRI observations of QSO OX 169, from Tananbaum (1980).

The condition that the size of the emitting region during a fluctuation, l , be smaller than $c \Delta t$ can be written as

$$\left(\frac{l}{10r_s}\right) < M_B^{-1} \left(\frac{\Delta t}{10^4 s}\right). \quad (10)$$

Since many of the fluctuations in Table 1 have $\Delta t \sim L$, we can assume that a large fraction of the steady emission region is involved in the observed fluctuations, $l \sim r$. Note that, within the context of the black hole model, equation (10) and Table 1 are consistent for $M_B \sim 0.1 - 10$. It is also important to note that if $M_B \sim 1$, and the fluctuations are produced at a radius $r \sim 10r_s$, the observed fluctuation timescales are shorter than an orbital period, cf.

equation (3). Since gravitational energy cannot easily be released on a timescale $\lesssim t_K$, the energy in an outburst must have been stored.

Some very general arguments may be given concerning the relation between L , ΔL , and Δt . By assuming that the energy in an outburst is produced by material that is associated with opacity, thereby increasing the light travel time across the emission region, Cavallo and Rees (1978) and Fabian and Rees (1979) have obtained the inequality

$$\Delta L < m_p c^4 \epsilon \Delta t / \sigma_T = 2 \times 10^{41} \text{ erg s}^{-1} \left(\frac{\epsilon}{0.1} \right) \Delta t. \quad (11)$$

By requiring that the steady luminosity be less than the Eddington limit and using equation (10), Lightman, Giacconi, and Tananbaum (1978) have pointed out the inequality

$$L < 10^{42} \text{ erg s}^{-1} \left(\frac{R}{10 r_s} \right)^{-1} \Delta t. \quad (12)$$

Fortunately (for theorists), none of the observations in Table 1 violate the above inequalities, although 3C 273 and NGC 6814 push them. That these inequalities seem to have something to do with the actual data suggest both high efficiencies, $\epsilon \gtrsim 0.1$, and an emission region of dimensions determined by the Schwarzschild radius of a black hole.

Clearly, long-term observations with large area detectors and high time resolution are desirable for further testing the above inequalities and related considerations. The proposed Large Area Modular Array of Reflectors (LAMAR) should be quite suitable for this task.

For time resolution sufficient to study a signal of magnitude $\Delta L/L \lesssim 0.1$, it may be possible to see large blobs of matter spiralling into the black hole. For a circular,

ORIGINAL PAGE IS
OF POOR QUALITY

non-spiralling orbit, we expect to see angular frequencies $\omega = (GM/r^3)^{1/2}$, in the Newtonian approximation, which can be written as

$$\omega = \omega_0 (r/r_0)^{-3/2} \quad (13a)$$

where $\omega_0 = 2\pi/P_0$ is the angular frequency at radius r_0 and P is given in equation (3). Now, for a radiating blob of matter that slowly spirals inward, the observed angular frequency will increase, seen as a low-Q quasi-periodicity, with decreasing period. To obtain an equation for this spiral, we may specify radius in terms of phase or azimuthal angle ϕ , and then integrate the relation $\omega = d\phi/dt$ along with equation (13a) to obtain $\phi(t)$. Signals would be modulated in proportion to $\cos\phi$.

The type of spiral depends on the local, nongravitational physics, particularly the viscous stresses. As a simple example, the "Archimedes spiral" is of the form

$$r = r_0 \left(1 - \frac{\phi}{2\pi n}\right)$$

where n is a free parameter, and yields

$$\phi(t) = 2\pi n \left[1 - \left(1 - \frac{5\omega_0 t}{4\pi n}\right)^{2/5}\right] \quad (13b)$$

Another spiral, which can be related to disk models in the literature, derives from equation (5a), $r^{-1}dr/d\phi = \beta$. If we assume that β is a constant (as given by a number of the α -disk models), then equation (5a) gives the logarithmic spiral

$$r = r_0 e^{-\beta\phi}$$

and yields

$$\phi(t) = \frac{2}{3\beta} \ln \left(1 - \frac{3\beta}{2} \omega_0 t\right)^{-1} \quad (13c)$$

We mention that simple analytic solutions may also be obta-

ined when β is a general power law in radius, rather than a constant. The above forms for ϕ are only applicable several Schwarzschild radii away from the black hole; similar general-relativistic expressions could be obtained closer to the hole.

Further theoretical work needs to be done on the time variability to be expected by matter inhomogeneities near the black hole. Accretion instabilities (Pringle, Rees, Pacholczyk 1973; Lightman and Eardley 1974; Shakura and Sunyaev 1976) may contribute to the observed variability. None of these possibilities has yet been modeled with sufficient detail, in the nonlinear regime, to make quantitative predictions.

D. Gas Supply

A clue to the environment of the power source might be gotten from study of the various sources of "fuel", the required conditions for these sources, and the different implications for luminosity evolution. Some of the models that have been proposed for the source of gas are (a) stellar collisions in a dense star system (e.g. Spitzer and Saslaw 1966), (b) tidal stripping of stars in a dense stellar system by a central massive black hole (Hills 1975), (c) infall of intergalactic gas (Gunn 1979), (d) galaxy mergers (e.g. Roos 1981), (e) intragalactic gas released by normal stellar evolutionary processes. One difficulty with models in which gas originates at large radii from the center is the necessity to dissipate a large amount of angular momentum. If the gas is provided by a dense stellar system, and if $M_g \gg 1$ and

$L \gg 10^{45} \text{ erg s}^{-1}$, then it can be shown that the dynamics of the stellar system must be dominated by physical stellar collisions (Shields and Wheeler 1978; McMillan, Lightman, and Cohn 1981).

It seems clear that substantial luminosity evolution occurs in QSOs (e.g. Turner 1979); AGN may be the late time phase of the same evolution. In principle, the gas supply mechanism should have something to do with luminosity evolution. The various mechanisms mentioned above, through their different dependences on the external environment of the QSO or AGN (in (c) and (d)), and on the internal parameters of the black hole and dense stellar system (in (a) and (b)), predict different functional forms for the evolving gas supply rate $\dot{M}(t)$, and hence for the evolving luminosity $L(t)$. A comparison of theoretical models for the gas supply mechanism with a large data set of received fluxes and redshifts might be able to rule out or partly confirm some of the models and clarify the relevant physical conditions. For example, models (a) and (b), with evolution of the stellar-system parameters included, yield late-time asymptotic laws of the form (McMillan, Lightman and Cohn 1981)

$$\dot{M}(t) \propto t^{-p}, \quad (14)$$

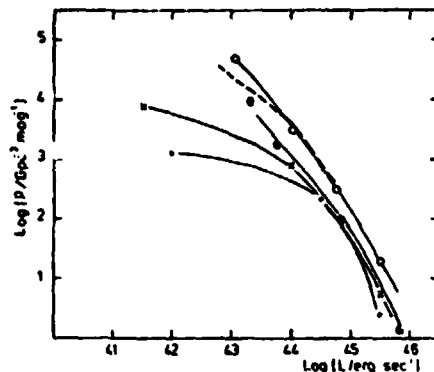
where $p=2$ for mechanism (a) and $p=1$ for mechanism (b).

The test of any theory of luminosity evolution is a statistical problem, requiring a value for the cosmological parameter q_0 , some information about the distribution of initial conditions or luminosities (the luminosity function), and some information about the distribution of "turn-on

times" of the objects -- in addition to an evolutionary law of the form of equation (14) for a single object. If additional assumptions can be made about these distributions, they may not need to be completely specified a priori. For example, Turner (1979) assumes the luminosity function maintains its shape in time, which, in our context, would allow determination of a value for p for every assumed value of q_0 . Unfortunately, Turner's assumption has little physical justification and seems to require some external clock that determines the physical conditions of each new quasar as it is born. In any case, a very dense X-ray Hubble diagram, with the fluxes and redshifts from many QSOs, will be necessary to solve the essentially statistical problem of luminosity evolution. X-rays seem particularly useful here, since QSOs may be readily identified by their X-ray emission, and this emission may constitute the majority of the total luminosity.

A good determination of the local luminosity function would be quite useful in the above project. Figure 2 below shows a luminosity function calculated for a number of nearby objects.

ORIGINAL PAGE IS
OF POOR QUALITY



- o X-ray luminosity function of Seyfert galaxies.
- Local, optical luminosity function of QSO's.
- Space density of Seyfert nuclei (optical).
- * Radio luminosity function of E+SO galaxies (1.4 GHz).
- + Radio luminosity function of E+SO cores (5 GHz).

Figure 2: Luminosity function of QSOs and AGN. The dashed line is fit from model (d) and additional assumptions. From Roos (1981).

The universality of the forms in Figure 2, especially above about $L = 3 \times 10^{43}$, suggests some universal type of process that establishes the range of conditions for QSOs and AGN.

III. RADIATION PROCESSES

A. Types of Mechanisms

It should be stated at the beginning that, while much of the emission in the radio is easily diagnosed as synchrotron radiation, there is little agreement on how the X-rays and gamma rays are produced. It is almost certain that the conditions in the X-ray emitting region are far from simple. A good fraction of the particles, especially those that ultimately form the observed jets, may be relativistic; there are accretion instabilities; shock waves and magnetic fields

ORIGIN
OF POOR QUALITY

abundant; the emission may be part thermal and part nonthermal. The radiation mechanisms we discuss can be divided into two categories: 1. Power-law electron models and 2. Non-power-law electron models. The second category can be further subdivided into thermal (random motions of electrons dominate emission) and nonthermal (bulk motions of electrons dominate emission) processes.

As will be shown below, the observed X-ray emission is well fit by a power law of the form

$$I_{\nu} \propto \nu^{-s}, \quad (15)$$

where I_{ν} is proportional to the energy per unit frequency ν .

1. Power-law electron models

If the X-ray emission is synchrotron radiation (requiring electron Lorentz factors $\gamma \sim 10^4$ for equipartition magnetic fields of $B \sim 10^4 G$) or relativistic inverse Compton, then a spectrum of the form of equation (15) can be achieved by a power law distribution of electrons of form

$$dn/d\gamma \propto \gamma^{-r} \quad (16a)$$

where

$$r = 2s + 1. \quad (16b)$$

For the observed values of the power-law index, $s \sim 0.7$, see below, we require $r \sim 2.4$. A number of groups (Axford, Leer and Skadron 1977, Bell 1978, Blandford and Ostriker 1978) have investigated first order Fermi mechanisms, whereby particles are accelerated into a power law distribution by the converging flows across a shock front. These mechanisms yield values $r \sim 2-3$, and have been applied to cosmic rays. It is also quite possible that such processes accelerate

electrons in the central regions of AGN and QSOs, where strong shocks may be present, and evidently produce an electron index in the appropriate range for synchrotron or inverse Compton radiation. If this is the nature of much of the radiation produced, then high X-ray polarization might be expected. Future X-ray polarization experiments may be quite important in clarifying this possibility.

2. Non-power law electron models

A power law spectrum can also be produced by the scattering of soft photons transmitted through a finite medium of hot electrons, even when these electrons do not themselves have a power-law distribution. In this case, a power law results from the absence of an energy scale over a large range of energy. When the electrons have a thermal, nonrelativistic distribution, then s may be related to the Thomson depth τ_{th} and temperature T (Shapiro, Lightman and Eardley 1976, Katz 1976) ($\tau_{th} > 1$)

$$s = -\frac{3}{2} + \left(\frac{9}{4} + \frac{4}{\gamma}\right)^{1/2}, \quad (17a)$$

where

$$\gamma \equiv 4T_* \tau_{th}^2 \quad (17b)$$

$$T_* \equiv kT/mc^2. \quad (18)$$

When the electrons have a thermal, relativistic distribution, then the corresponding result is (Pozdnyakov, Sobol and Sunyaev 1976) ($\tau_{th} < 1$)

$$s = \ln \tau_{th}^{-1} / \ln (16 T_*^2) \quad (19)$$

We mention that power laws may also be produced by the above process for non-thermal electrons, as long as their distribution is sharply peaked at some "effective temperature." Takahara (1980), Takahara, Tsuruta and Ichimaru (1981) and Maras-

chi, Roasio and Treves (1981) have recently considered models using the above radiation mechanism. The soft photons for this process could be generated by cyclotron radiation (Eardley and Lightman 1976; Takahara, Tsuruta and Ichimaru 1981), produced at perhaps 10^{10} Hz and absorbed up to about the 100th harmonic. Soft photons could also be produced by cold dense clouds in pressure equilibrium with the hot phase of the plasma.

A problem with the Comptonization mechanisms above is that the spectral index depends on the parameters τ_{th} and T , which might be expected to vary from one source to another, in contradiction with the narrow range of s actually observed (see D. below). For a scattering model to work in this context, a "characteristic" geometry or structure is required. For example, if the soft photons are externally incident on a region of hot, thermal electrons with a large scattering depth, then the reflected X-rays have a more universal spectrum. Lightman and Rybicki (1979a) have investigated this process and obtain the universal quasi-power law (for $\nu \gg \nu_0$)

$$s = \frac{3}{2} \left(\ln \frac{\nu}{\nu_0} \right)^{-1}, \quad (20)$$

where ν_0 is the typical frequency of the soft photon input. This power law extends up to photon energies $h\nu \sim kT$ and into the relativistic domain if the electrons have relativistic random motions.

In the above scattering mechanisms, it is the random motion of the electrons that dominates the emission. A closely related mechanism that depends on the bulk electron motion is

ORIGINAL PAGE IS
OF POOR QUALITY

the scattering of initially soft photons by the converging flows across a shock front. This process has been investigated by Blandford and Payne (1981a, 1981b) and gives a high energy asymptotic result

$$s = (M^2 - 1/2) (M^2 + 6) (M^2 - 1)^{-2}, \quad (21)$$

where M is the Mach number of the shock (not to be confused with a mass). This power law extends up to frequencies such that the photon momentum equals that of the electron. Thus, the bulk motions must be relativistic to produce photons of energies $h\nu \gtrsim mc^2$. Since characteristic bulk velocities are only of the order $v \sim 0.3c$ at $r \sim 10 r_g$, this scattering process may have difficulty in producing relativistic photons. In any case, Equation (20) gives a value of s a little too small and equation (21), for a strong shock, $M \gg 1$, gives a value of s a little too large. It is possible that refinements of these models might be more satisfactory.

Some general statements may be made. Any thermal process must result in a characteristic thermal (exponential) turnover in the spectrum, and possibly a Wien hump, at $h\nu \sim kT$. A shock mechanism should have a cutoff in the spectrum at energies $h\nu \sim mc(\gamma v)_{shock}$. In almost all cases, no turnovers of any kind have yet been seen. It is important to extend X-ray observations up to higher energies, in search of such a turnover. In any case, it is clear that some turnover must occur, since the observed value of $s \sim 0.7$ indicates an infinite total energy if this power law continues to arbitrarily high frequencies.

Changes of the spectrum during luminosity fluctuations

may also provide some information about the emission mechanism. In any scattering model in which soft photons are scattered up to high energies, one expects the spectrum to harden during a fluctuation if the temperature remains constant. Rybicki and Lightman (1979b) and Payne (1980) have investigated the time-dependent versions of Comptonization by thermal electrons within this context. Some attempts have been made to model the observed (or absence of) spectral evolution in outbursts by such processes (e.g. Tennant et al. 1981). If the Compton cooling time is much shorter than the energy input time, it may be the soft photon source rather than the temperature that remains constant during fluctuations. Guilbert, Ross and Fabian (1981) have investigated this possibility and find that the spectrum first hardens and then softens as the temperature decreases. Over a range of parameters with $\gamma \gg 1$, the time-averaged spectrum has a quasi power-law shape, with $0 < s < 1$, and a thermal cutoff (with no Wien hump) at the initial electron temperature. It is possible that in many cases, steady state spectra are not relevant and we should always be considering time averages of nonsteady processes. Better spectral resolution during luminosity fluctuations will be helpful here.

There are various processes that may be involved in producing the electron distribution, if it is not thermal. In addition to the shock acceleration already mentioned, large scale magnetic and electric fields may be present (Blandford 1976, Lovelace 1976, Blandford and Znajek 1977). Cavaliere and Morrison (1980) have pointed out that the electrons must

be reaccelerated in crossing the emission region. Defining a parameter q by

$$q = \left(\begin{array}{l} \text{probability} \\ \text{of scattering} \end{array} \right) \times \left(\begin{array}{l} \text{fractional energy loss} \\ \text{per scattering} \end{array} \right) \quad (22)$$

$$= (\sigma_T n_\gamma r) \times (\gamma^2 h\nu / \gamma mc^2).$$

Here n_γ is the photon density

$$n_\gamma = L / (4\pi r^2 c h\nu), \quad (23)$$

so that

$$q \sim 70\gamma \left(\frac{L}{L_{\text{Edd}}} \right) \left(\frac{r}{10r_s} \right)^{-1}. \quad (24)$$

In any source where q exceeds unity, reacceleration is necessary. Note that q is about equal to the Kepler time divided by the Compton cooling time.

B. Thermalization Time Scales

A principal uncertainty is whether any of the observed X-ray emission from QSOs and AGN is thermal. Such emission requires that the electrons be able to thermalize, via two-body collisions or perhaps collective plasma motions, on a time scale shorter than energy is deposited or radiated and shorter than pair creation when the latter is important. We will consider two-body thermalization below, keeping in mind that collective effects may always be faster.

First we consider the ion thermalization time. The bulk of the released gravitational energy is probably initially deposited into the ions. Taking a value of 25 for the Coulomb logarithm, the ion thermalization time, t_{ii} , via ion-ion scattering is, cf. Spitzer (1962)

$$t_{ii} = (3kT)^{3/2} m_p^{1/2} (5.6\pi N e^4 \ell_r \Omega)^{-1} = 5 \times 10^{17} \text{ s } N^{-1} \left(\frac{T}{10^{12} \text{ K}} \right)^{3/2}. \quad (25a)$$

Substituting equation (6) into equation (25a), and taking $T =$

ORIGINAL PAGE IS
OF POOR QUALITY

10^{12} K, we obtain

$$t_{ii} = 5 \times 10^7 \text{ s} \left(\frac{L}{L_{\text{EDD}}} \right)^{-1} \beta \left(\frac{\epsilon}{0.1} \right) M_8, \quad (25b)$$

and using equations (3) and (5b), we obtain

$$t_{ii}/t_r = 1.6 \times 10^2 \left(\frac{L}{L_{\text{EDD}}} \right)^{-1} \beta^2 \left(\frac{\epsilon}{0.1} \right). \quad (25c)$$

Here and elsewhere in this section, all quantities will be evaluated at $r=10r_g$ for simplicity, unless otherwise stated. Since energy is deposited into the ions on a timescale t_r , the last ratio must be less than unity for ion-ion collisions to thermalize the ions. Ions may also thermalize by scattering with the electrons. If we denote this timescale by t_{ie} , then

$$t_{ii}/t_{ie} \sim \left(\frac{m}{m_p} \right)^{1/2} \left(\frac{n_- + n_+}{N} \right) \left(\frac{m}{m_p} + \frac{T_e}{T_i} \right)^{-3/2}, \quad (26)$$

where T_i and T_e denote the ion and electron temperature, respectively. (If the particles are not thermal, then temperatures should be replaced by mean energies.) For $T_i = 10^{12}$ K and $T_e = mc^2 = 6 \times 10^9$ K, equation (26) gives $t_{ii}/t_{ie} \sim 50 (n_- + n_+)/N$. Thus, a relatively low electron mean energy and the presence of many electron positron pairs may allow the ions to thermalize.

Next we consider electron thermalization via electron-electron scattering. For relativistic electrons, $T_e \gg 1$, this timescale, t_{ee} , is

$$\begin{aligned} t_{ee} &= T_e^2 (n_- + n_+)^{-1} (c \sigma_T \ln \Lambda)^{-1} \\ &= 2.4 \times 10^2 \text{ s} T_e^2 \left(\frac{n_- + n_+}{N} \right)^{-1} \left(\frac{L}{L_{\text{EDD}}} \right)^{-1} \beta \left(\frac{\epsilon}{0.1} \right) M_8. \end{aligned} \quad (27)$$

The electron cooling time, t_{cool} , may be evaluated in a model-independent way:

$$t_{\text{cool}} \equiv \frac{4}{3} \pi r^3 (n_- + n_+) (3kT) / L = T_x \left(\frac{n_- + n_+}{N} \right) \left(\frac{m}{m_p} \right) (\beta \epsilon)^{-1} t_K. \quad (28)$$

We then obtain the ratio

$$t_{\text{ee}} / t_{\text{cool}} \sim 0.1 T_x \left(\frac{N}{n_- + n_+} \right)^2 \left(\frac{L}{L_{\text{EDD}}} \right)^{-1} \beta^2 \left(\frac{\epsilon}{0.1} \right)^2, \quad (29)$$

which must be less than unity for the electrons to thermalize. Equation (29) suggests that in some cases we might expect thermal electrons and in some cases not. As long as the electrons are only marginally relativistic, the electrons should be able to thermalize unless the luminosity is very much below the Eddington limit and there are few electron positron pairs. It seems likely, however, that a fraction of the electrons will be accelerated up to very relativistic energies by some of the processes mentioned above. In this case we would not expect the electrons to be able to sustain a thermal distribution. In any event, as is discussed below, the copious production of e^+e^- pairs prevents the temperature of an optically thin thermal medium from becoming very relativistic.

The time scale for electrons to receive energy from ions, t_{ei} , satisfies

$$t_{ei} = t_{ie} \left(\frac{T_e}{T_i} \right) \left(\frac{n_+ + n_-}{N} \right)$$

Since electrons can cool relatively efficiently, faster than they receive energy from the ions, we may expect the electron mean energy to be much lower than that of the ions, as suggested by Shapiro, Lightman and Eardley (1976).

The conclusion is that there may well be two populations of electrons: a marginally relativistic, thermal population and a highly relativistic, nonthermal population. Unfortunately, it is difficult to calculate the relative proportions of these two populations at the present time.

ORIGINAL PAGE IS
OF POOR QUALITY

C. Pair Effects

With the high virial temperatures available, cf. equation (2), much exceeding the electron rest mass, it seems likely that some sizeable fraction of the electrons will be at least marginally relativistic, and most detailed models in the literature (e.g. Shapiro, Lightman and Eardley 1976; Maraschi, Roasio and Treves 1981; Takahara, Tsuruta and Ichimaru 1981) do indeed have this character. In such a situation, the effects of electron-positron pair production must be included. When pairs are present, the distributions of radiation and pairs must be solved for self consistently, since photons produce pairs, pairs produce photons, and all the cross sections are, in general, energy dependent. Some recent work in these processes has been done for steady plasmas by Stoeger (1977), Liang (1979), Lightman and Band (1981), Lightman (1981), and Svensson (1981), and in the context of a time-dependent cooling "fireball" by Cavallo and Rees (1978).

As an example, we consider production of pairs by the reaction



which may dominate when a large photon density is present and the electrons are energetic. This reaction gives a positron production rate

$$\dot{n}_{+} \sim C \sigma_T \alpha_F n_{\gamma} (n_{+} + n_{-}) \quad (30)$$

(where α_F is the fine structure constant), only logarithmically sensitive to the particle and photon distributions, as long as the threshold condition

ORIGINAL PAGE IS
OF POOR QUALITY

$$\gamma h\nu > mc^2$$

is strongly satisfied. The pair production time scale for this process, $t_{pe\gamma}$, is

$$t_{pe\gamma} \equiv n_+/\dot{n}_+ = .06 t_r \beta \left\langle \frac{h\nu}{mc^2} \right\rangle \left(\frac{L}{L_{EDD}} \right)^{-1} \left(\frac{r}{10r_g} \right)^{1/2} \left(\frac{n_+}{n_+ + n_-} \right), \quad (31)$$

where we have used equations (23), (5b) and (3), and the L refers to the luminosity in those photons above threshold. In sources that are not too far below the Eddington limit, we therefore expect this process to have ample time to produce pairs. Since pairs produce more pairs, there may be a non-steady behavior in which, for a short period of time (and with n_γ varying rapidly perhaps), an overabundance of pairs is produced.

It is also of interest to compare the time scale, t_{ann} , for the pair annihilation process



to the cooling time. (In a steady state the creation time would equal the annihilation time.) If pairs cool before they annihilate, then we might expect to see a feature in the spectrum at the electron rest mass energy, as has been seen (redshifted by 20%) in the March 1979 gamma ray burst event. For QSOs at redshift z , this feature would be at the energy $511 \text{ keV}/(1+z)$. For electrons of Lorentz factor γ ,

$$t_{ann} = 16\gamma^2 / (27\sigma_T c n_-). \quad (32)$$

In addition to comparing equation (32) to equation (28) we can assume a specific cooling mechanism. For example, the time scale for synchrotron cooling, t_{syn} , is

$$t_{syn} = 6\pi mc / (\gamma B^2 \sigma_T). \quad (33)$$

Then, using the expression for the gas and magnetic pres-

ORIGINAL PAGE IS
OF POOR QUALITY

tures, P_G , and P_B , respectively,

$$P_G = \frac{1}{3} \gamma mc^2 (n_- + n_+) \quad (34)$$

$$P_B = B^2/8\pi, \quad (35)$$

we can obtain the ratio

$$t_{\text{syn}}/t_{\text{ann}} = 3\gamma^{-4} (P_G/P_B). \quad (36)$$

For equipartition magnetic fields, $P_B \sim P_G$, pairs will evidently cool before they annihilate as long as $\gamma \geq 2$. The absence of an observed annihilation line may indicate the magnetic fields are below their equipartition value. When relativistic pairs annihilate before substantial cooling, the photons produced will at most yield a broad feature at $h\nu \sim \gamma mc^2$, and even this may be dominated by Comptonized bremsstrahlung radiation (Lightman and Band 1981).

Recent work (Lightman 1981; Svensson 1981) has shown that there is a maximum temperature that can be achieved by a thermal, optically thin plasma in equilibrium, dependent on the value of the ion scattering depth, equation (7). A maximum temperature comes about because the pair annihilation rate decreases with increasing temperature and the pair production rate increases as the photon density increases (which increases with τ_N). This maximum (or, equivalently, the maximum τ_N possible for each value of T) is shown in Figure 3. Furthermore, there is generally an enormous range in luminosity over which the temperature remains in the narrow range $0.1 \lesssim T_* \lesssim 1$, with copious pair production at the high end and threshold effects at the low end serving as a thermostat.

ORIGINAL PAGE IS
OF POOR QUALITY

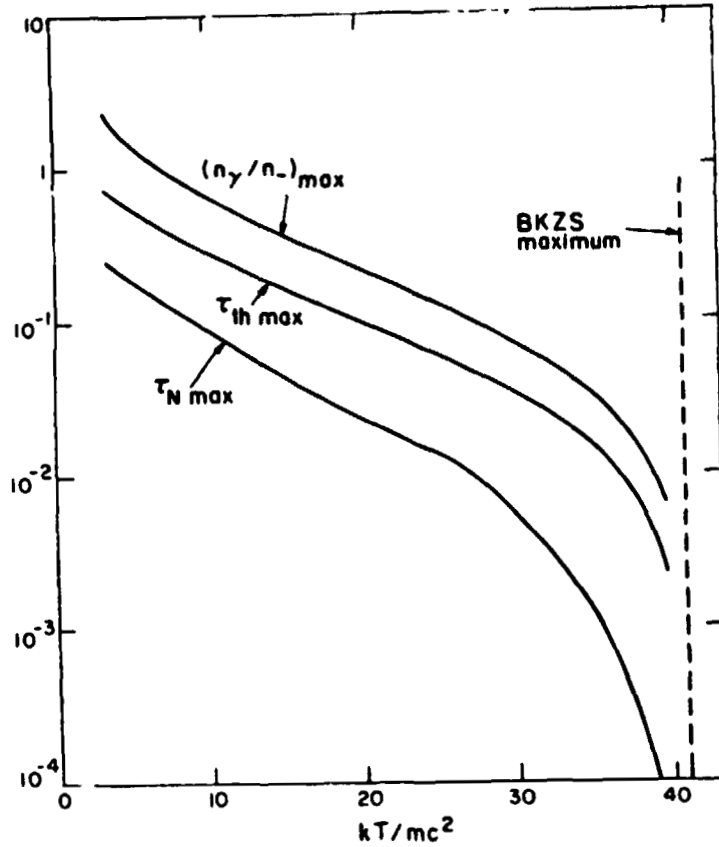


Figure 3: Maximum ion scattering depth, Thomson depth, and photon to electron ratio that can be achieved at each temperature in an optically thin, steady thermal plasma. From Lightman (1981).

Earlier work by Bisnovatyi-Kogan, Zeldovich, and Sunyaev (1971), which did not include finite size effects and neglected photon processes, obtained the maximum temperature $kT=41mc^2$. The magnitude of this maximum is set by the reciprocal of the fine structure constant. In the calculations resulting in Figure 3, only internal sources of photons were included (bremsstrahlung, double Compton, and annihilation). Any additional source of photons, e.g. a soft photon source, must lower the maximum T at each value of τ_N , since photons

ORIGINAL PAGE IS
OF POOR QUALITY

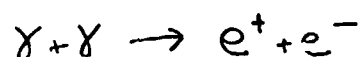
produce but do not destroy pairs in an optically thin plasma. Thus, the maxima shown in Figure 3 are upper limits. Observed spectra with power laws extending above $h\nu > kT_{\max}$ indicate that either the plasma is nonthermal or nonsteady.

Another constraint on the mean energy and number density of the pairs arises from requiring that the total system of ions and pairs must be gravitationally confined. This leads to the inequality

$$\gamma \left(\frac{n_- + n_+}{N} \right) < \frac{1}{4} \left(\frac{m_p}{m} \right) \left(\frac{r}{r_s} \right)^{-1} . \quad (37)$$

When equation (37) is violated, magnetic confinement requires magnetic fields above equipartition strength. Equation (37) must be satisfied on average, but could be violated for short times or over small regions.

We finally mention that photon-photon pair production



may limit the presence of hard gamma rays. If $h\nu_s$ is the energy of a soft photon and $h\nu_h$ is the energy of a hard photon, then the threshold condition for pair production is

$$\left(\frac{h\nu_s}{mc^2} \right) \left(\frac{h\nu_h}{mc^2} \right) \gg 2$$

The scattering depth to the above reaction is

$$\tau_{\gamma\gamma} = n_s \sigma_T r \quad (38)$$

where n_s is the number density of "field" photons in a bandwidth $2\nu_s$ around ν_s . Some constraints may be placed on sources for which strong gamma emission is seen, by requiring that the number density n_s be sufficiently small to achieve $\tau_{\gamma\gamma} < 1$, (Herterich 1974). For example, Fabian and Rees (1979) have shown that the observed gamma and X-ray emission

from 3C 273 (see Figure 4) require that the gamma rays be emitted in a region $r > 10^{18}$ cm, much larger than the X-ray emitting region. We mention, however, that the above constraint may be violated if the produced pairs themselves produce more gamma rays that are not substantially downgraded in energy. Since the various reactions that would redistribute the spectrum, e.g. Compton scattering, are energy dependent, it is not clear how large $\tau_{\gamma\gamma}$ can be before the gamma rays would certainly be cut off. This is an area in which more research is needed.

D. Observed Spectra

The composite spectrum of the QSO 3C 273 is shown in Figure 4.

ORIGINAL PAGE IS
OF POOR QUALITY

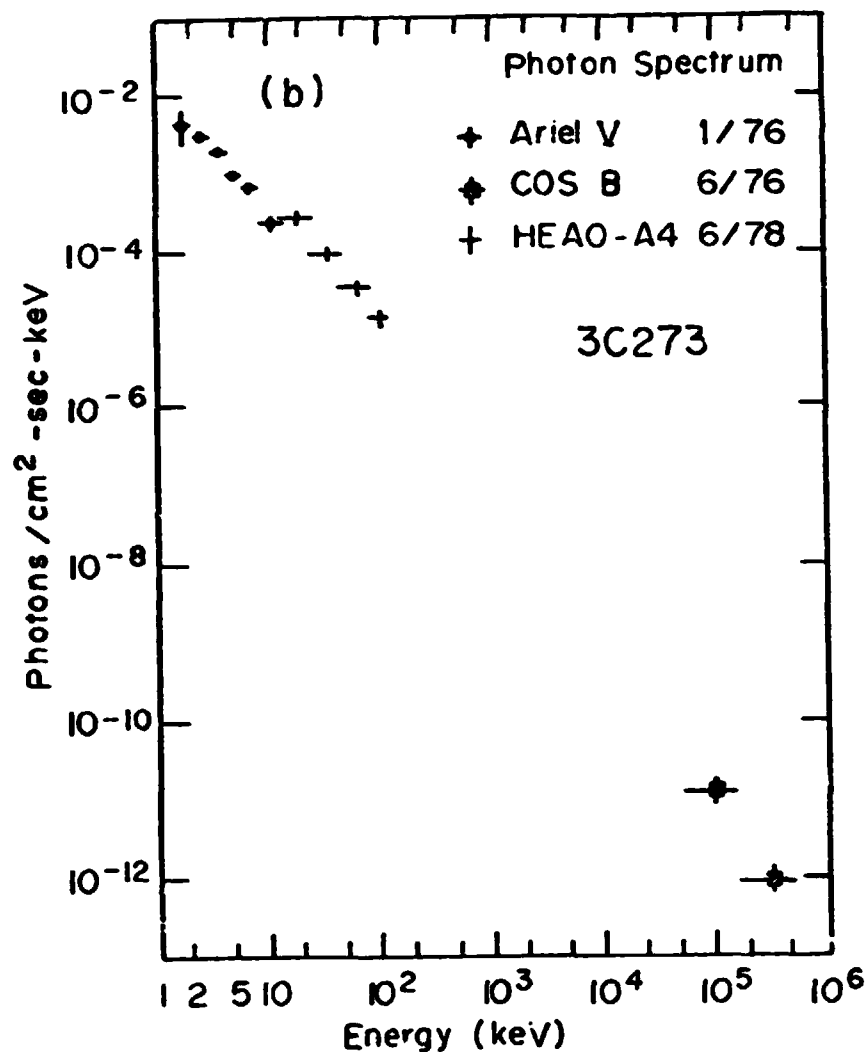


Figure 4: Spectrum of 3C 273. From Bradt (1980)

The portion of this spectrum from 13 to 120 keV is well fit by a power law with $s=0.67$. This spectrum is actually fairly characteristic of many AGN and QSOs. In Figure 5, we see a histogram of spectral indices that describe power laws seen in Seyfert galaxies. (The index α in Figure 5 is the same as the s given in equation (15).)

ORIGINAL PAGE IS
OF POOR QUALITY

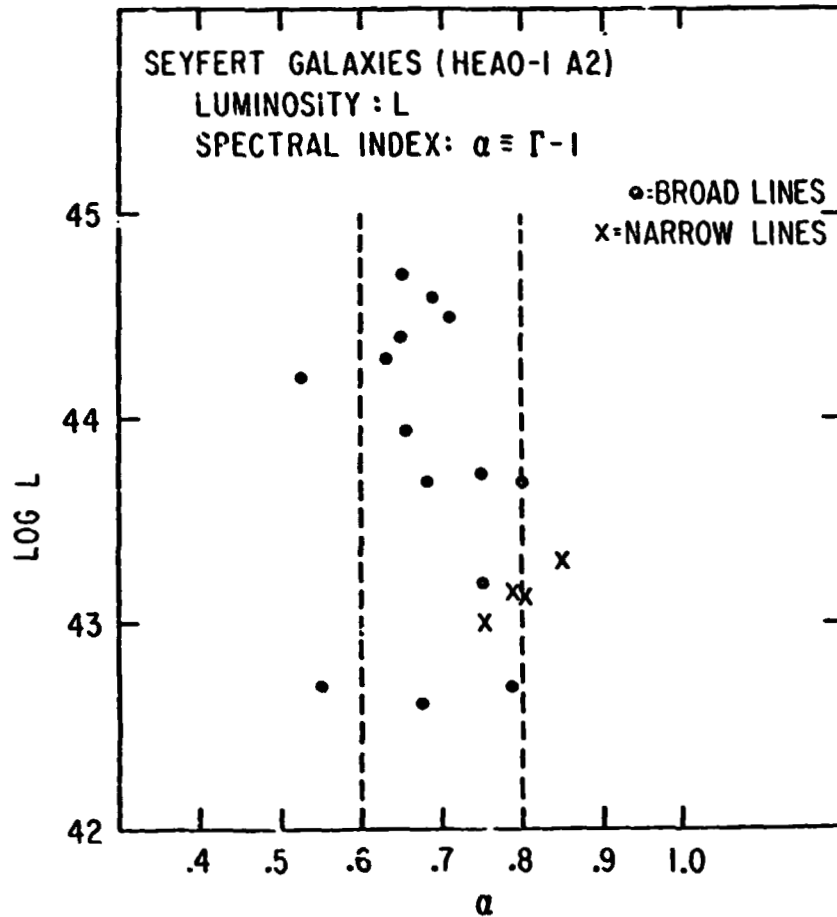


Figure 5: Histogram of spectral indices observed for Seyfert galaxies. α is the energy index. From Mushotzky (1981).

The data, over an observed range 1-100 keV, are well fit with an $s \sim 0.69$, and a small scatter about this mean $\sigma \sim 0.15$. This result has been reported by Mushotzky (1981) and by Maccauro, Perola and Elvis (1981). The universality of these spectra is striking and suggests a universal type of emission mechanism, as discussed above. Emission above 1 MeV has also been seen in a few other objects, e.g. NGC 4151 (Schonfelder 1978). It is crucial to obtain spectra of as many QSOs as possible, to confirm the similarity of their spectra to those

of AGN. For t' s purpose large area detectors like LAMAR should be useful.

From all the above considerations, there is a clear need for observations at higher energies, going into the gamma rays. There may be a wonderland of interesting physics waiting to be learned at $h\nu \geq mc^2$. The proposed satellite GRO should have such a capability. To summarize the needs for such observations:

(1) With a spectral index of $s=0.7$, most of the total luminosity has yet to be observed! Look back at all the go-or-no-go formulae that contain an L. Until the observations are pushed to sufficiently high energies to see a turnover in the spectrum, we only have lower limits on that L.

(2) When a break, or turnover, in the spectrum is seen at high energies, we will have a much better idea of whether the emission is thermal or nonthermal.

(3) As suggested by the discussion in C. above, a number of interesting effects associated with electron-positron pairs may be seen at energies $h\nu \geq mc^2$. These features and the physical effects they represent may be completely hidden at lower energies.

Observations of the spectra at low energies, especially near the soft X-ray absorption cutoff, $h\nu \lesssim 1$ keV, are also important. Lawrence and Elvis (1981) have recently found good evidence for a correlation between total X-ray luminosity and the ratio of hard ($h\nu = 2-10$ keV) to soft ($h\nu = 0.5-4.5$ keV) components. They interpret this result to indicate that the covering factor of the broad line emission

region over the continuum X-ray source is a monotonically decreasing function of X-ray luminosity. Two possible explanations are that brighter sources, either through radiation pressure or hydrodynamic effects, are able to "blow away" the surrounding absorbing gas, or that the accumulation of absorbing gas is associated with ageing (e.g. through stellar evolutionary processes) and older objects are in the declining phase of their activity (see luminosity evolution in II D. above).

IV. BEAMS AND JETS

It is impossible to consider the subject of QSOs and AGN without mentioning the dramatic, well collimated streams of matter seen emanating from the centers of these objects. These "jets" have been detected in a variety of different objects and in several different wavelengths. Recently, they have been seen in the X-ray band also (e.g. Schreier et. al. 1979, Feigelson et. al. 1981). The opening angle of a jet is typically $\theta \lesssim 10^\circ$, the velocity of the matter $300 \text{ km s}^{-1} < v < c$, and the jet lifetime $t_{\text{jete}} \gtrsim 10^6 \text{ yr}$. See Rees (1980) and Begelman, Blandford and Rees (1981) for recent reviews of the physics of jets.

Since jets are ubiquitous in QSOs and AGN, whatever produces a jet should be a commonly occurring phenomenon, not requiring special conditions. Furthermore, the jet "remembers" its directionality for a million years or more, so the fundamental beaming mechanism must be associated with a longlived and stable axis of symmetry. Most researchers feel that net

ORIGINAL PAGE IS
OF POOR QUALITY

angular momentum is a key ingredient in defining the required axis, but the detailed mechanism for accelerating matter along this axis is not yet understood.

One of the earliest suggestions was the "twin-exhaust" hydrodynamic model of Blandford and Rees (1974), in which a heat source at the center of a rotating gas cloud, in an external gravitating potential, creates a low density channel of gas that burrows a tunnel along the path of least resistance, the rotation axis. The first detailed hydrodynamical calculations to test the validity of this suggestion have recently been completed by Norman et. al. (1981), and some of their results are shown in Figure 6.

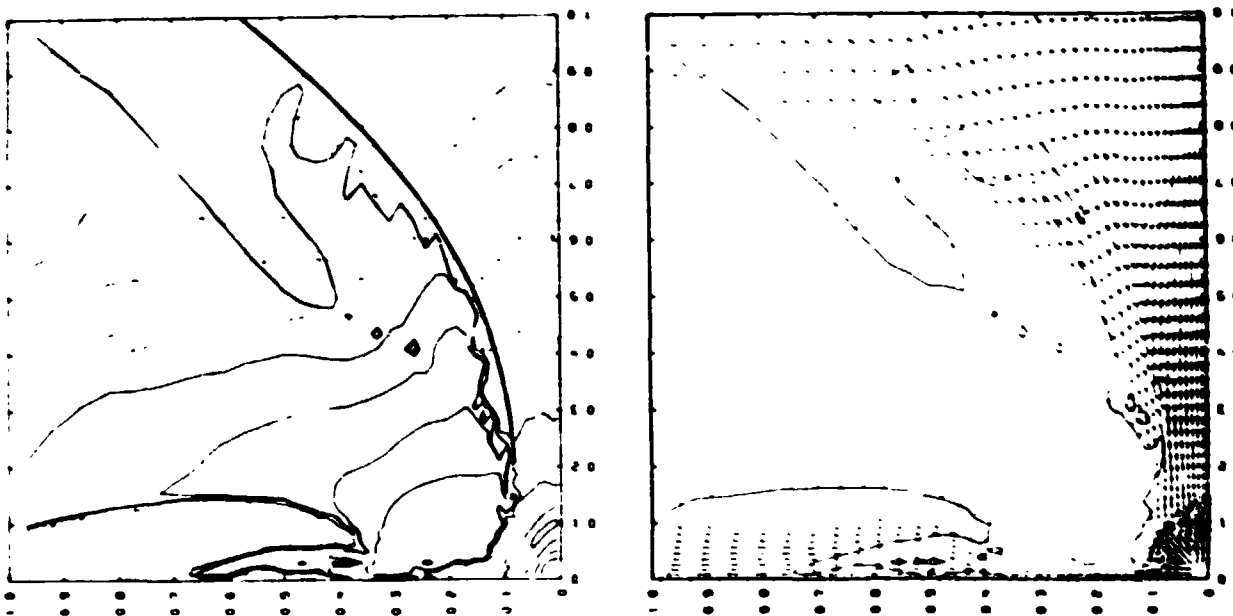


Figure 6a: Density contours of the cloud jet structure at $t=1.6$. The solid line is the jet wall. The rotation axis is vertical. Units given in the text. From Norman et. al. (1981).

Figure 6b: The velocity vector field for the jet in 6a. Note the central shock. From Norman et. al. (1981).

The unit of length here is GM/c^2 , where M is the mass of the confining cloud and c is the internal energy per unit mass of the hot, light gas introduced at the center. The unit of time is GM/c^3 . The central cavity is at a radius $R=0.15$. The gas accelerates smoothly to supersonic velocity, terminating in a shock front at $R=0.1$, at which point collimation begins. These results indicate a cavity-nozzle structure more compact than that suggested by Blandford and Rees (1974). The calculations of Norman et. al. (1981) assume a flat bottomed gravitational potential, rather than a point source potential that would be generated by a central black hole. Future such calculations, perhaps more applicable to the AGN and QSO context, will yield one of the first reliable estimates for the amount of collimation that may be achieved by this mechanism.

Another idea, suggested by Lynden-Bell (1978), is that radiation pressure may accelerate matter along the interior funnel formed by a thick accretion disk (e.g. Jaroszynski, Abramowicz and Paczynski 1980). Some recent kinematical studies by Abramowicz and Piran (1980) suggest that the disk funnel must be extremely narrow for this method to yield adequate collimation, with a ratio of outer to inner disk radii of at least 10^4 . No calculations have yet been done to self consistently determine the parameters of the funnel, or to test whether such a narrow funnel is stable in the presence of radiation and matter.

It is quite possible that none of the above mechanisms are able to achieve the observed collimation, and that much

of the collimation is actually achieved far from the black hole, perhaps by large scale magnetic fields. Blandford and Payne (1981c) have recently investigated such a model, in which angular momentum is removed from an accretion disk by magnetic fields that extend to large radii. An outflow of matter along the rotation axis is then possible. At large distances from the disk, the toroidal component of the magnetic field may collimate the matter.

V. CONCLUSIONS

We conclude by recapping some of the important future observations that may clarify the physics of QSOs and AGN.

1. Temporal Resolution. (a) The various theoretical constraints on L , ΔL , and Δt , when pushed to their limits, may provide our best handles on the efficiencies and emission-region sizes. (b) Spectral changes during fluctuations may help specify the radiation mechanism. (c) Signatures of spiralling matter or accretion instabilities may be revealed by high time resolution.

2. Large Sample of QSO Spectra, Intensities, and Redshifts. (a) It is important to learn whether a single universal spectrum describes QSOs as well as AGN. (b) With a large X-ray Hubble diagram for QSOs, we can begin to test luminosity evolution against theoretical models of the gas supply mechanism.

3. X-ray Polarization. Synchrotron radiation typically produces large polarization. Most other mechanisms produce a small polarization.

4. High Energy Measurements $h\nu \sim 1-10$ MeV. (a) With an observed spectral index $S \sim 0.7$ for AGN, we now have only a lower bound on the total luminosity of most of these objects. (b) The shape of the turnover in the spectrum, at high energies, should tell us about the emission mechanism. (c) A good deal of physics associated with pair production (maximum temperatures of thermal, steady plasmas; annihilation features) can only be observed at energies $h\nu \gtrsim 1.02$ MeV.

To end with a note of caution: Most of the ideas have been presented as if there were one universal framework for all QSOs and AGN, one basic scenario of gas accretion onto a massive black hole, one dominant radiation process, one mechanism for producing and collimating the jets. I think sometimes, especially in astronomy, we tend to use Occam's razor too much. We should be receptive to the possibility that a number of different processes and mechanisms may be operating in different objects, or perhaps going on simultaneously in the same object -- even though the net results of luminosities, spectra, and variabilities can be squeezed into a common framework.

Acknowledgments

We thank D. Eardley, M. Elvis, P. Gorenstein, J. Grindlay, D. Payne, G. Rybicki, and H. Tananbaum at the Harvard-Smithsonian Center for Astrophysics for useful comments. This work was supported in part by NASA grant NAGW 246.

REFERENCES

- Abramowicz, M.A. and Piran, T. 1980, *Ap. J. Lett.*, 241, 17.
- Angel, R. 1978, in *Proc. Pittsburg Conference on BL Lac Objects*,
ed. A.M. Wolfe
- Axford, W.I., Leer, E., and Skadron, G. 1977, *Proc. 15th Int.
Cosmic Ray Conference (Plovdiv, Bulgaria)*.
- Bardeen, J. and Petterson, J.A. 1974, *Ap. J. Lett.*, 195, L65.
- Begelman, M.C., Blandford, R.D. and Rees, M.J. 1981, *Ann.
N.Y. Acad. Sci.*, in press.
- Bell, A.R. 1978, *M.N.R.A.S.*, 182, 147.
- Bisnovatyi-Kogan, G.S., Zeldovich, Ya.B., and Sunyaev, R.A.
1971, *Sov. Astr.-AJ*, 15, 17.
- Blandford, R.D. 1976, *M.N.R.A.S.*, 176, 465.
- Blandford, R.D. and Ostriker, J.P. 1978, *Ap. J. Lett.*, 221, L29.
- Blandford, R.D. and Payne, D.G. 1981a, *M.N.R.A.S.*, 194, 1033.
- Blandford, R.D. and Payne, D.G. 1981b, *M.N.R.A.S.*, 194, 1041.
- Blandford, R.D. and Payne, D.G. 1981c, preprint.
- Blandford, R.D. and Rees, M.J. 1974, *M.N.R.A.S.*, 169, 395.
- Blandford, R.D. and Znajek, P.L. 1977, *M.N.R.A.S.*, 179, 433.
- Bradt, H.V. 1980, *Ann. N.Y. Acad. Sci.*, 336, 59.
- Cavaliere, A. and Morrison, P. 1980, *Ap. J. Lett.*, 238, L63.
- Cavallo, G. and Rees, M.J. 1978, *M.N.R.A.S.* 183, 359.
- Delvaille, J.P., Epstein, A. and Schnopper, H.W. 1978,
Ap. J. Lett., 219, L81.

- Eardley, D.M. and Lightman, A.P. 1976, *Nature*, 262, 196.
- Eardley, D.M., Lightman, A.P., Payne, D.G. and Shapiro, S.L.
1978, *Ap. J.*, 224, 53.
- Fabian, A.C. and Rees, M.J. 1979, in *X-ray Astronomy*, ed.
W.A. Baity and L.E. Peterson (Pergamon).
- Feigelson, E.D., Schreier, E.J., Delvaille, J.P., Giacconi, R.,
Grindlay, J.E. and Lightman, A.P. 1981, *Ap J.*, in press.
- Guilbert, P.W., Ross, R.R. and Fabian, A.C. 1981, *M.N.R.A.S.*
in press.
- Gunn, J.E. 1979, in *Active Galactic Nuclei*, ed. C. Hazard and
S. Mitton (Cambridge University Press).
- Heterich, K. 1974, *Nature*, 250, 311.
- Hills, J.G. 1975, *Nature*, 254, 295.
- Jaroszynski, M., Abramowicz, M.A. and Paczynski, B. 1980,
Acta Astr., 30,
- Katz, J.I. 1976, *Ap J.*, 206, 910.
- Lawrence, A. and Elvis, M. 1981, *Ap. J.*, in press.
- Liang, E.P.T. 1979, *Ap. J.*, 234, 1105.
- Lightman, A.P. 1981, *Ap. J.*, in press.
- Lightman, A.P. and Band, D. 1981, *Ap. J.*, in press.
- Lightman, A.P. and Eardley, D.M. 1974, *Ap. J. Lett.*, 187, L1.
- Lightman, A. P., Giacconi, R. and Tananbaum, H., 1978,
Ap. J., 224, 375.
- Lightman, A.P. and Rybicki, G.B. 1979a, *Ap J. Lett.* 229, L15.
- Lightman, A.P. and Rybicki, G.B. 1979b, *Ap. J.*, 232, 882.

- Lovelace, R.V.E. 1976, *Nature*, 262, 649.
- Lynden-Bell, D. 1978, *Phys. Scripta*, 17, 185.
- Maccajaro, T., Perola, G.C., and Elvis, M. 1981, *Ap. J.*,
in press.
- Maraschi, L., Perola, G.C., Reina, C. and Treves, A. 1979,
Ap. J., 230, 243.
- Maraschi, L., Roasio, R. and Treves, A. 1981, *Ap. J.*, 1981,
in press.
- McMillan, S.L.W., Lightman, A.P. and Cohn, H. 1981, *Ap. J.*,
in press.
- Mushotzky, R.F. 1981, *Ap. J.*, in press.
- Mushotzky, R.F., Holt, S.S. and Serlemitsos, P.J. 1978, *Ap. J.*
Lett., 225, L115.
- Norman, M.L., Smarr, L. Wilson, J.R. and Smith, M.D. 1981,
Ap. J., 247, 52.
- Payne, D.G. 1980, *Ap. J.*, 237, 951.
- Pozdnyakov, L.A., Sobol, I.M. and Sunyaev, R.A. 1976, *Sov.*
Astron. Lett., 2, 55.
- Pringle, J.E., Rees, M.J. and Pacholczyk, A.G. 1973, *Astr. Ap.*,
29, 179.
- Rees, M.J. 1977, *Ann. N.Y. Acad. Sci.*, 302, 613.
- Rees, M.J. 1978, *Phys. Scripta*, 17, 193.
- Rees, M.J. 1980, in *Origin of Cosmic Rays*, ed. G. Setti,
and A. Wolfendale (Reidel).
- Ricketts, M.J., Cooke, B.A. and Pounds, K.A. 1976, *Nature*,
259, 546.

- Roos, N. 1981, PhD thesis, University of Leiden.
- Schonfelder, V. 1978, *Nature*, 274, 344.
- Schreier, E. et al. 1979, *Ap. J. Lett.*, 23, L30.
- Shakura, N.I. and Sunyaev, R.A. 1973, *Astr. and Ap.*, 24, 337.
- Shakura, N.I. and Sunyaev, R.A. 1976, *M.N.R.A.S.*, 175, 613.
- Shapiro, S.L., Lightman, A. P. and Eardley, D.M. 1976, *Ap. J.*, 204, 187.
- Shields, G.A. and Wheeler, J.C. 1978, *Ap. J.*, 222, 667.
- Spitzer, L. 1962, *Physics of Fully Ionized Gases*, (John Wiley and Sons: new York)
- Spitzer, L. and Saslaw, W.C. 1966, *Ap. J.* 143, 400.
- Stein, W.A., O'Dell, S.L. and Strittmatter, P.A. 1976, *Ann. Rev. Astr. Ap.*, 14, 173.
- Stoeger, W.R. 1977, *Astr. Ap.*, 61, 659.
- Svensson, R. 1981, preprint.
- Takahara, F. 1980, *Prog. Theo. Phys.*, 63, 1551.
- Takahara, F., Tsuruta, S. and Ichimaru, S. 1981, *Ap. J.*, in press.
- Tananbaum, H. 1980, in *X-ray Astronomy*, ed. R. Giacconi and G. Setti (Reidel).
- Tananbaum, H., Peters, G., Forman, W., Giacconi, R. and Jones, C. 1978, *Ap. J.*, 223, 74.
- Tennant, A.F., Mushotzky, R.F., Boldt, E.A. and Swank, J.H. 1981, *Ap. J.*, in press.
- Turner, E. 1979, *Ap.J.*, 231, 231.
- Winkler, P.F. and White, A.E. 1975, *Ap. J. Lett.*, 199, L139.